

# **Analysis of amorphous-nanocrystalline silicon thin films by Time-of-Flight Elastic Recoil Detection Analysis and High-Resolution Electron Microscopy**

D. Gracin<sup>1</sup>, Z. Siketić<sup>1</sup>, K. Juraić<sup>1</sup> M. Čeh<sup>2</sup>

<sup>1</sup>Ruđer Bošković Institute, Zagreb, Bijenička c. 54, Croatia

<sup>2</sup>Jozef Štefan Institute, Ljubljana, Jamova 11, Slovenia

The in-depth distribution of hydrogen atoms in 100-nm-thick, amorphous-nanocrystalline, silicon films (a-nc-Si:H) was estimated by Time-of-Flight Elastic Recoil Detection Analysis (TOF-ERDA) using a previously described set-up. The layer with nanocrystals was deposited on a 50-nm amorphous layer by Plasma Enhanced Chemical Vapor Deposition (PECVD), using silane gas that was diluted with hydrogen. High-Resolution Transmission Electron Microscopy (HRTEM) showed that the films contained nanocrystals of silicon embedded in an amorphous Si:H matrix. The size of the nanocrystals and the crystal-to-amorphous ratio increased in the direction from the substrate towards the surface of the film. The amorphous matrix appeared uniform, except for the area close to the a-Si:H/a-nc-Si:H interface, where spots that were brighter than average appeared. These areas can be attributed to the presence of less-dense material, presumably voids. It is assumed that the surface of the voids is “decorated” with hydrogen that saturates the silicon “dangling bonds”. This is why the distribution of hydrogen should indicate a density fluctuation in the material. Consistent with this assumption, the TOF-ERDA showed a non-uniform distribution of hydrogen across the depth, with a maximum value close to the a-Si:H/a-nc-Si:H interface that coincides with the less-dense material seen by the HRTEM. This supports the idea about the important influence of voids on crystal formation, particularly in the nucleation phase. After a heat treatment at 400°C, the distribution of hydrogen remained the same, while the total hydrogen concentration decreased. This indicated that the type of hydrogen bonding was the same across the amorphous network and assumed that the areas of less-dense material are agglomerates of smaller voids.

Corresponding Author: Krunoslav Juraić  
Ruđer Bošković Institute, Bijenička c. 54, 10000 Zagreb, Croatia  
Telephone: +385 1 4560790  
Fax: +385 1 4680114  
E-mail: [kjuraic@irb.hr](mailto:kjuraic@irb.hr)

# **Analysis of amorphous-nanocrystalline silicon thin films by Time-of-Flight Elastic Recoil Detection Analysis and High-Resolution Electron Microscopy**

D. Gracin<sup>1</sup>, Z. Siketić<sup>1</sup>, K. Juraić<sup>1</sup>, M. Čeh<sup>2</sup>

<sup>1</sup>Ruđer Bošković Institute, Zagreb, Bijenička c. 54, Croatia

<sup>2</sup>Jozef Štefan Institute, Ljubljana, Jamova 11, Slovenia

The in-depth distribution of hydrogen atoms in 100-nm-thick, amorphous-nanocrystalline, silicon films (a-nc-Si:H) was estimated by Time-of-Flight Elastic Recoil Detection Analysis (TOF-ERDA) using a previously described set-up. The layer with nanocrystals was deposited on a 50-nm amorphous layer by Plasma Enhanced Chemical Vapor Deposition (PECVD), using silane gas that was diluted with hydrogen. High-Resolution Transmission Electron Microscopy (HRTEM) showed that the films contained nanocrystals of silicon embedded in an amorphous Si:H matrix. The size of the nanocrystals and the crystal-to-amorphous ratio increased in the direction from the substrate towards the surface of the film. The amorphous matrix appeared uniform, except for the area close to the a-Si:H/a-nc-Si:H interface, where spots that were brighter than average appeared. These areas can be attributed to the presence of less-dense material, presumably voids. It is assumed that the surface of the voids is “decorated” with hydrogen that saturates the silicon “dangling bonds”. This is why the distribution of hydrogen should indicate a density fluctuation in the material. Consistent with this assumption, the TOF-ERDA showed a non-uniform distribution of hydrogen across the depth, with a maximum value close to the a-Si:H/a-nc-Si:H interface that coincides with the less-dense material seen by the HRTEM. This supports the idea about the important influence of voids on crystal formation, particularly in the nucleation phase. After a heat treatment at 400°C, the distribution of hydrogen remained the same, while the total hydrogen concentration decreased. This indicated that the type of hydrogen bonding was the same across the amorphous network and assumed that the areas of less-dense material are agglomerates of smaller voids.

## **Introduction**

Amorphous-nanocrystalline silicon (a-nc-Si:H) is a promising material for thin-film solar cells. It could be a satisfactory replacement for pure amorphous silicon due to it suffering from much less degradation during exposure to light. Furthermore, nanocrystals, 2–10 nm in size, show quantum size-effects and offer further possibilities for tailoring the optical gap and the increased use of such material in multilayer solar cells [1-3]. An additional interesting fact is that the material can be obtained in a highly crystalline form (a crystal fraction of 70% and above) by plasma-enhanced chemical vapor deposition in silane that is diluted with hydrogen gas on a substrate heated to 200–300 °C. In the modeling of the nanocrystals formation the most important role has been ascribed to the atomic hydrogen formed in the glow discharge. In contact with the surface of the growing film, the hydrogen atoms etch away the less-well-bonded silicon in less-ordered domains and in this way promote the formation of a more-ordered material. The diffusivity of the atomic hydrogen is large, and that is why the near-surface layer becomes enriched with hydrogen, presumably in voids, so increasing the high compressive stresses. The consequence of such stresses is the generation of strained Si–Si bonds, which accelerates the nucleation of crystallites. As a result, the crystals grow in a highly strained and void-rich a-Si layer [4-7]. According to the above-mentioned model, the initial layer should contain voids and a larger concentration of hydrogen than the average for the film. In order to check this assumption, we deposited an amorphous-nanocrystalline silicon layer on a 50-nm amorphous layer. The a-Si:H/a-nc-Si:H interface was studied with High-Resolution Electron Microscopy (HRTEM), while the distribution of hydrogen in the bi-layer was measured with Time-of-Flight Elastic Recoil Detection Analysis (TOF-ERDA). The growth of the a-nc-Si:H layer was selected to be relatively slow (2 nm/min), leaving enough time for the process of hydrogen incorporation. The results obtained from this experiment should be valid for all other depositions of this kind under a variety of conditions.

## **Experimental**

The samples were deposited by Plasma-Enhanced Chemical Vapor Deposition using a radio-frequency discharge in a gas mixture of silane (90%) and hydrogen (10%) for the amorphous layer, while the dilution was increased to 94% hydrogen in a gas mixture for the formation of a-nc-Si:H [8]. The substrate was glass and glass covered with a SnO<sub>2</sub> thin film. The power density

during the formation of the a-nc-Si:H layer was  $20 \text{ mW/cm}^2$ , resulting in a film growth rate of 2 nm/min. The sample thickness was 60 nm. The thermal treatment was conducted in a vacuum at  $400^\circ\text{C}$  for 1 hour. The crystallinity of the deposited layers was estimated using Raman spectroscopy [9]. The typical values were between 30 and 40% of crystal phase. The HRTEM measurements were performed using a JEOL JEM 2010F transmission electron microscope. Details of the HRTEM experiment and the sample preparation are given in Ref. [9]. The HRTEM images were filtered with a FFT filter using a Bragg mask in order to emphasize the ordered (crystalline) domains of the sample. The size of the nanocrystals was taken as the diameter of the circle with the area of the nanocrystal taken from a micrograph [10].

The atomic content and the depth profiles of the hydrogen and silicon in the samples were determined using TOF-ERDA. The TOF-ERDA measurements were performed on the 6-MV Tandem Van de Graaff accelerator located at the Ruđer Bošković Institute. As shown in Fig. 1, 20-MeV  $^{127}\text{I}^{7+}$  ions with a  $10^\circ$  incidence angle, with respect to the sample surface, were used. The TOF-ERDA spectrometer was positioned at an angle of  $37.5^\circ$  to the beam direction. T1 and T2 are the timing stations for measuring the time of flight and E is the energy detector. More details about the TOF-ERDA spectrometer and the method can be found in Ref. [11, 12].

## Results and discussion

### HRTEM

A characteristic micrograph of the a-nc-Si:H sample is shown in Fig.2. It is clear that the nanocrystals exhibit various sizes and orientations, and are isolated and immersed in the amorphous silicon matrix. The mean size of the crystals was about 7 nm, while the distribution was log-normal, indicating random nucleation (Fig. 3). The number of nanocrystals formed close to the interface was much smaller than the number formed close to the surface of the film.

The micrographs in Fig.4 show a cross-section of the a-nc-Si:H deposited on a-Si:H for the TCO layer. The square indicates the area where the film appears less dense than the a-Si:H and a-nc-Si:H. These areas extend close to the interface between the two layers and appear at the beginning of the a-nc-Si:H formation. After the formation of the a-Si:H layer, the film growth continued in the silane diluted with up to 94% of hydrogen in the gas mixture. As a consequence

of the dilution the plasma that came into contact with the surface of the growing film contained a lot of neutral and ionized hydrogen atoms that impinged on the surface of the grown film. Part of this flux was spent on chemical etching of the less-ordered material, while part of the hydrogen penetrated below the surface, into the grown film, creating the defects that enable faster diffusion of the atoms. As a consequence of this hydrogen incorporation, it is also possible that the larger voids appeared and filled up with hydrogen. Such defects could enhance the formation of a strained Si-Si bond and the formation of nucleation centers for the crystallization. Besides nanocrystal growth on the top of the amorphous layer, incorporated hydrogen also creates a favorable situation for the formation of nanocrystals in the already-formed a-Si:H matrix. One such crystal is visible in the micrograph of the a-Si:H/a-nc-Si:H interface shown in Fig.5. The amorphous phase is on the left-hand side of the figure. The small crystal formed at about 10–15 nm from the interface is indicated by an arrow.

### **TOF-ERDA**

The TOF-ERDA coincidence map of the as-deposited sample is shown in Fig.6. Data belonging to each element (mass) were selected and analyzed using well-known relations between the energy and the depth, and between the number of events and the atomic content (slab analysis). The results of the analysis, i.e., the elemental depth profiles, of the as-deposited and heat-treated samples are shown in Fig.7 as a) and b), respectively. The estimated depth was about  $500 \times 10^{15}$  Si at/cm<sup>2</sup> for a 110-nm thickness of the Si layer for both samples, which means that the void density was about 10%. The elemental depth profiles of the as-deposited (7a) and heat-treated (7b) samples look very similar, except that the hydrogen concentration is lower in the heat-treated sample. The hydrogen concentration across the depth of the sample is more clearly seen in Fig. 8. In this case the analysis of the spectra (the hydrogen depth profile) was performed using the simulation code SIMNRA [13]. In the as-deposited amorphous layer (Fig 8a) the hydrogen concentration was about 5% close to substrate, while at the interface with the nanocrystalline layer it increased to about 11%. In the a-nc-Si:H layer the concentration of hydrogen again decreased in the direction from the interface towards the surface of the layer. This decrease is possible as a consequence of the crystal formation, which increased from the interface towards the surface. Most of the hydrogen in the a-nc-Si:H layer is located in the amorphous material and, possibly, on the surface of the crystals. This means that the amorphous

part of the a-nc-Si:H layer contains some 30–40% more hydrogen than the pure amorphous layer. The maximum in the hydrogen concentration coincides with the bright spots in the HRTEM micrographs, which supports the assumption of nano-voids filled with hydrogen. Also, the hydrogen concentration in the a-Si:H layer is greater closer to the interface as a consequence of the hydrogen penetration during the a-nc-Si:H formation. The hydrogen concentration is lower when closer to the surface, possibly as a consequence of the increase in the contribution of the crystals in the film. The distribution of the hydrogen concentration across the film after the heat treatment (8b) looks very similar to that in the as-deposited film (8a), except that the maximum at the interface is not so pronounced. Since hydrogen effuses from the film much more easily from the large voids than from the small ones. However, the similarities in the hydrogen profiles suggest that the large voids are not dominant in the film. The less-dense material at the a-Si:H/a-nc-Si:H interface is most probably just agglomerates of small voids.

## **Conclusion**

An a-nc-Si:H layer was formed using PECVD on top of an amorphous layer. The samples were examined by HRTEM and TOF-ERDA. It was found that the concentration of hydrogen is non-uniform and that it has a maximum value at the a-Si:H/a-nc-Si:H interface. It also decreased towards the substrate and the surface of the bi-layer. The maximum in the hydrogen concentration corresponded to bright spots in the HRTEM images that could be a part of the sample that is rich in voids filled with hydrogen. Such a structure supports the model where the initial crystallization in the a-nc-Si:H layer is aided by an increasing number of defects close to the surface of the growing film and the pressure caused by the accumulation of hydrogen in the voids.

The hydrogen concentration after the heat treatment at 400°C in vacuum was much lower than the concentration in the as-deposited sample, while the shape of the distribution remained the same. This assumes that the less-dense material, seen with the HRTEM, consisted of agglomerates of small voids.

## **Acknowledgment**

This work was supported by the Croatian Ministry of Science Education and Sport through the Unity through Knowledge Fund (UKF), Grant Agreement no. 68/10, grants “The thin film silicon on the amorphous to crystalline transition” (098-0982886-2894) and “Physics and applications of nanostructures and bulk matter” (098-0982904-2898).

## Literature

- [1] M.A. Green, Potential for low dimensional structures in photovoltaics, *Materials Science and Engineering B-Solid State Materials for Advanced Technology* 74 (1–3) (2000) 118–124.
- [2] M.A. Green, Third generation photovoltaics: solar cells for 2020 and beyond, *Physica E-Low-Dimensional Systems and Nanostructures* 14 (1–2) (2002) 65–70.
- [3] D. Gracin, A. Gajović, K. Juračić, M. Čeh, Z. Remeš, A. Poruba, M. Vaneček, Spectral response of amorphous-nanocrystalline silicon thin films, *Journal of Non-Crystalline Solids* 354 (2008) 19-25.
- [4] H. Fujiwara, M. Kondo, and A. Matsuda, Stress-Induced Nucleation of Microcrystalline Silicon from Amorphous Phase, *Japanese Journal of Applied Physics*, 41 (2002) 2821-2828.
- [5] H. Fujiwara, M. Kondo, and A. Matsuda, Microcrystalline silicon nucleation sites in the sub-surface of hydrogenated amorphous silicon, *Surface Science* 497 (2002) 333-340.
- [6] M. W. M. van Cleef, J. K. Rath, F. A. Rubinelli, C. H. M. van der Werf, R. E. I. Schropp, and W. F. van der Weg, Performance of heterojunction p+ microcrystalline silicon n crystalline silicon solar cells, *Journal of Applied Physics* 82 (1997) 6089-6096.
- [7] J. K. Rath and R. E. I. Schropp, Incorporation of p-type microcrystalline silicon films in amorphous silicon based solar cells in a superstrate structure, *Sol. Energy Mater. Sol. Cells* 53 (1998) 189-203.
- [8] D. Gracin, S. Bernstorff, p. Dubcek, A. Gajovic, K. Juraic, Study of amorphous nanocrystalline thin silicon films by grazing-incidence small-angle X-ray scattering, *Journal of Applied Crystallography* 40 (2007) S373–S376.
- [9] A. Gajović, D. Gracin, K. Juračić, J. Sancho-Parramon, M. Čeh, Correlating Raman-spectroscopy and high-resolution transmission-electron-microscopy studies of



amorphous/nanocrystalline multilayered silicon thin films, *Thin Solid Films* 517 (18) (2009) 5453–5458.

[10] A. Gajović, D. Gracin, I. Djerdj, N. Tomašić, K. Jurać, D. Sheng Su, Nanostructure of thin silicon films by combining HRTEM, XRD and Raman spectroscopy measurements and the implication to the optical properties, *Applied Surface Science* 254 (9) (2008) 2748–2754.

[11] Z. Siketić, I. Bogdanović Radović, M. Jakšić: Development of a time-of-flight spectrometer at the Ruđer Bošković Institute in Zagreb, *Nuclear Instruments and Methods in Physics Research, Section B* 266 (2008) 1328

[12] Z. Siketić, I. Bogdanović Radović, M. Jakšić: Quantitative analysis of hydrogen in thin films using TOF ERDA spectroscopy, *Thin Solid Films* 518 (2010), 2617-2622

[13] M. Mayer, Technical Report IPP 9/113, Max-Planck Institut für Plasmaphysik, Garching, Germany, 1997.

## Figure captions

**Fig.1** TOF-ERDA experimental setup

**Fig.2.** HRTEM micrograph of a-nc-Si:H sample (as deposited). The boundaries of several nanocrystals are highlighted.

**Fig.3** Characteristic nanocrystal size distribution obtained from HRTEM micrograms by FFT filtering and a mathematical fit of the obtained data to a log-normal size distribution.

**Fig.4** Micrograph of a-Si:H/a-nc-Si:H interface with visible bright areas, possibly a less-dense part of the material

**Fig.5** Micrograph of a-Si:H/a-nc-Si:H interface; the nanocrystal formed in the a-Si:H area is indicated by an arrow.

**Fig.6** TOF-ERDA coincidence map of the a-nc-Si:H sample (as deposited)

**Fig.7.** Elemental analysis of the as-deposited sample (a) and the heat-treated sample (b)

**Fig.8** Depth distribution of hydrogen in the as-deposited (a) and heat-treated sample (b)

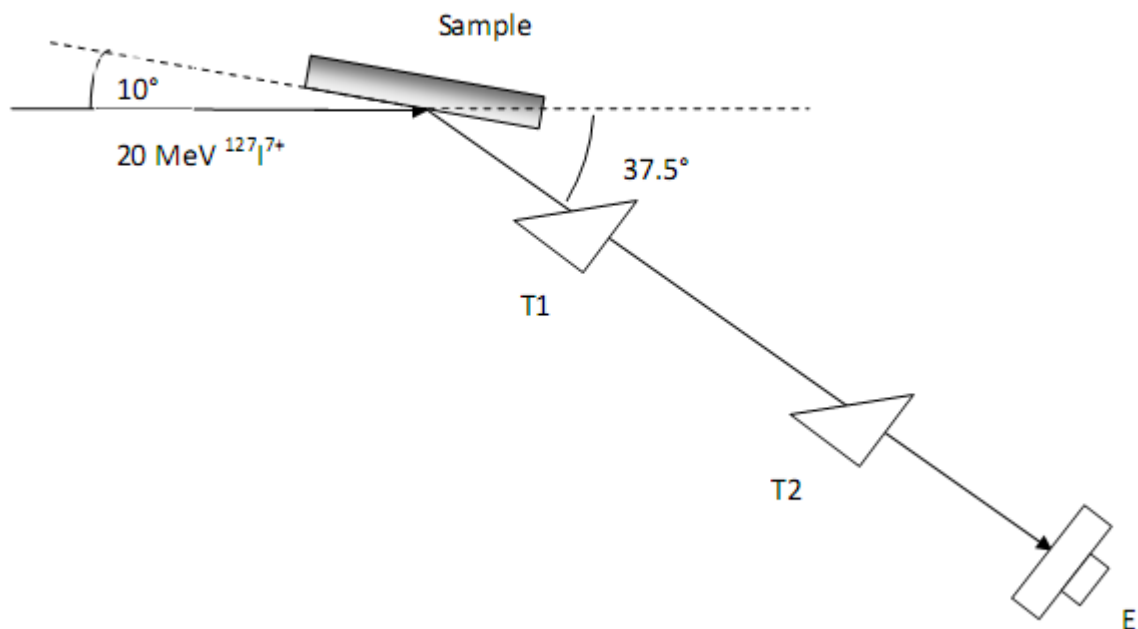


**Fig. 1**

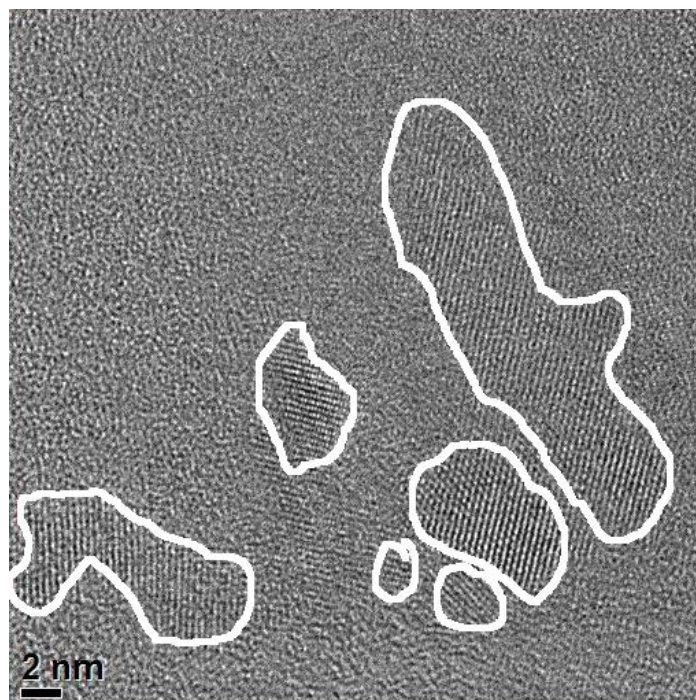


**Fig 2**

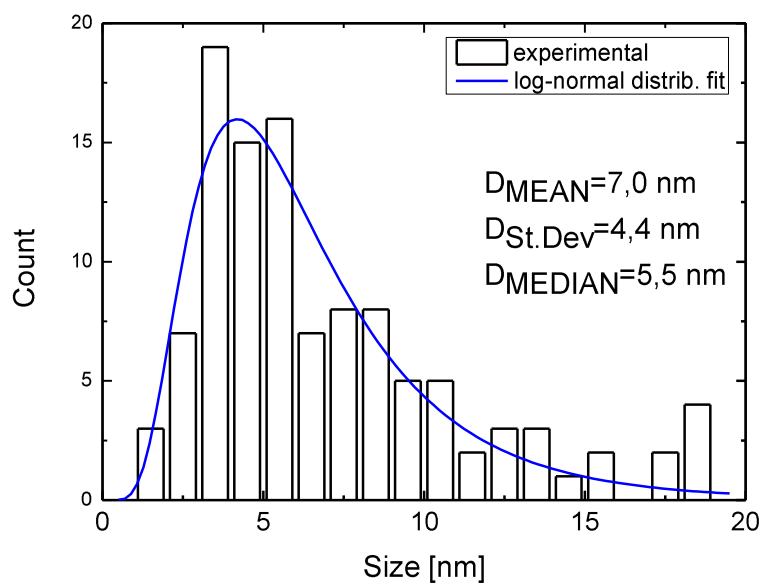


**Fig. 3**

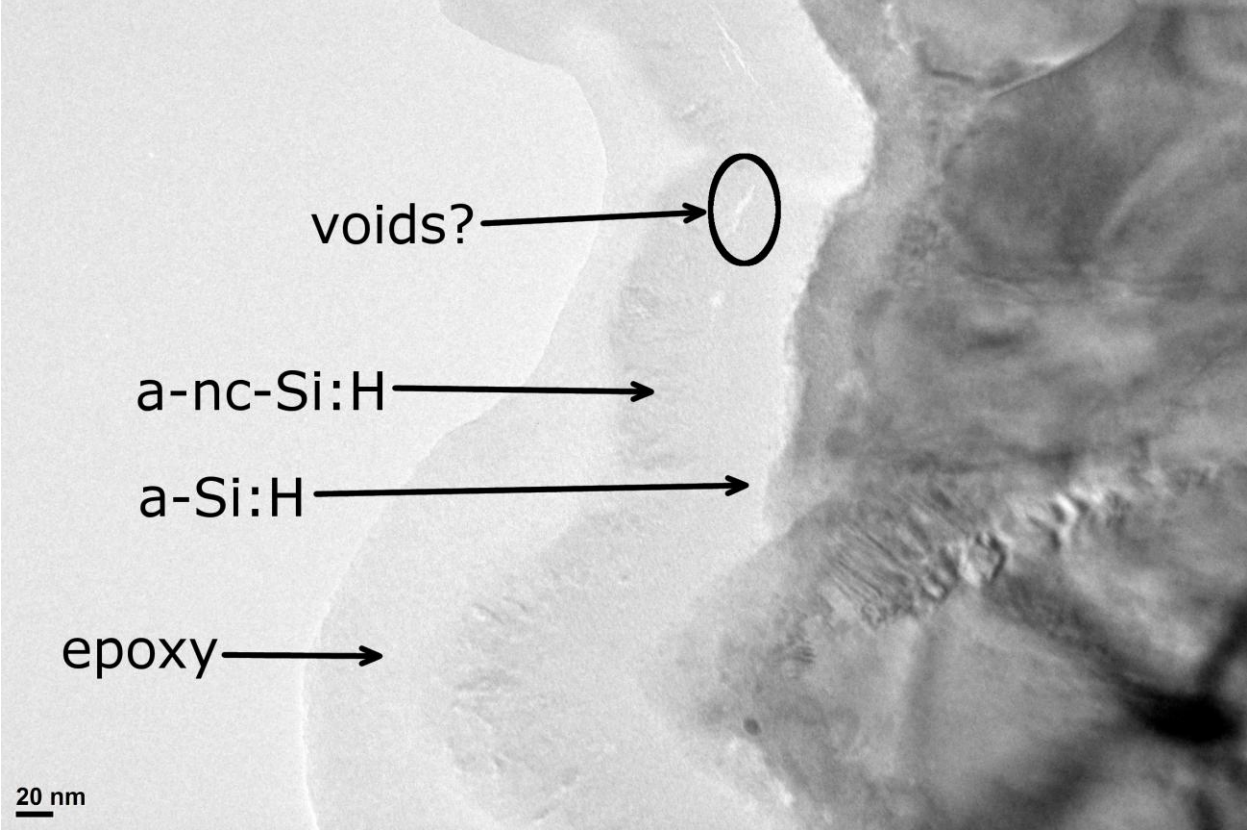


Fig. 4

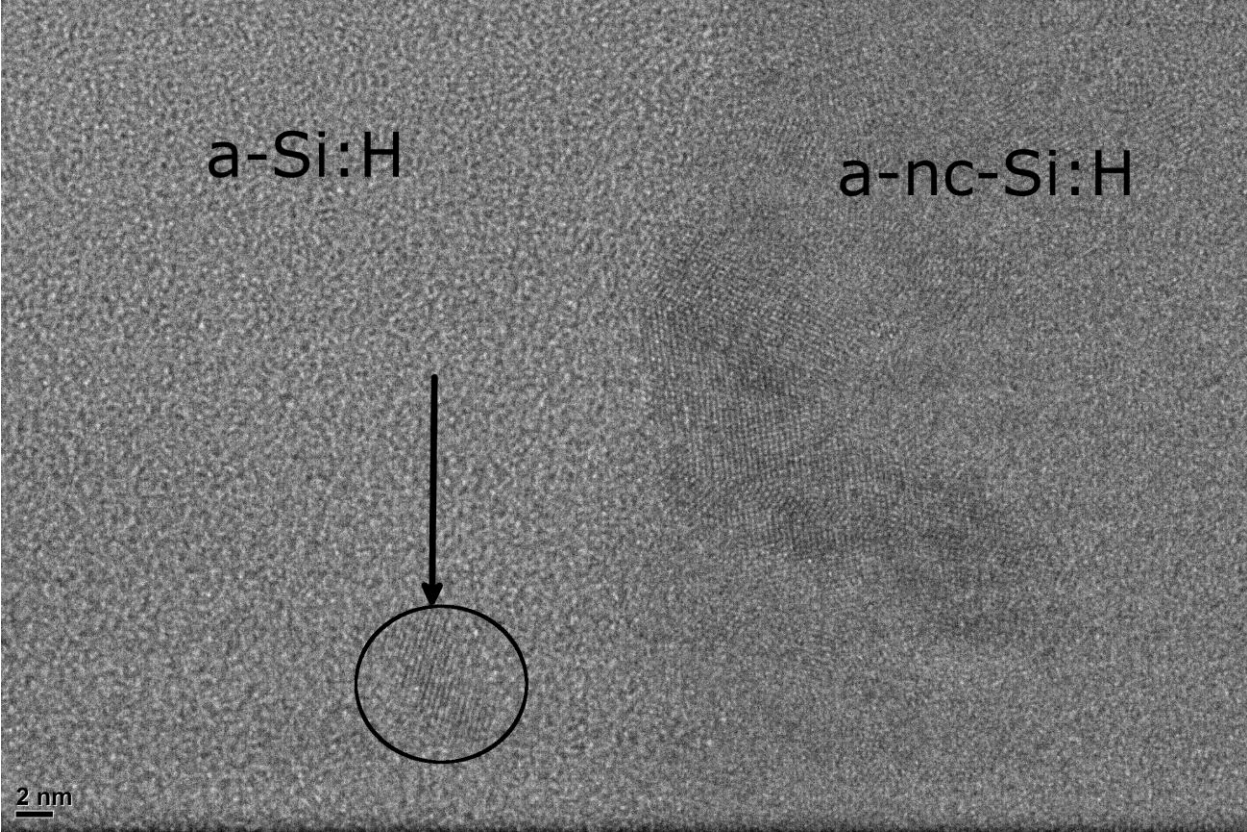


Fig. 5

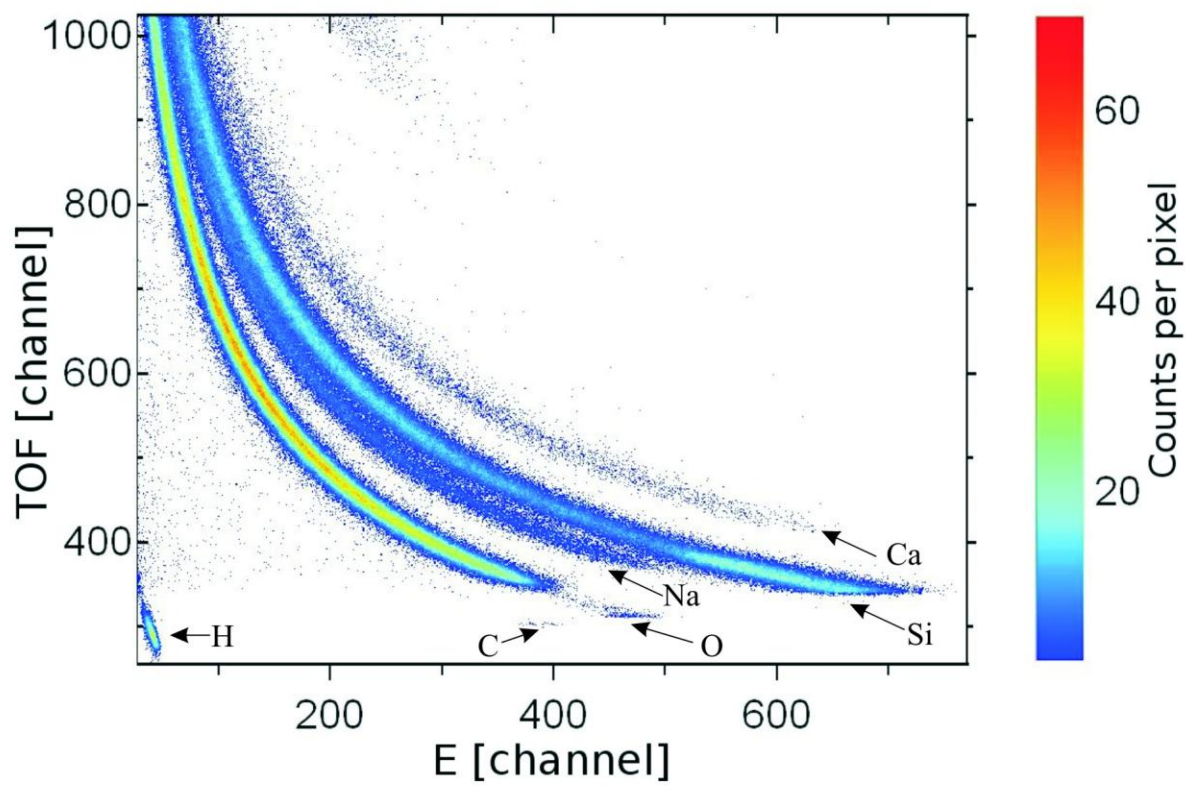


Fig 6.

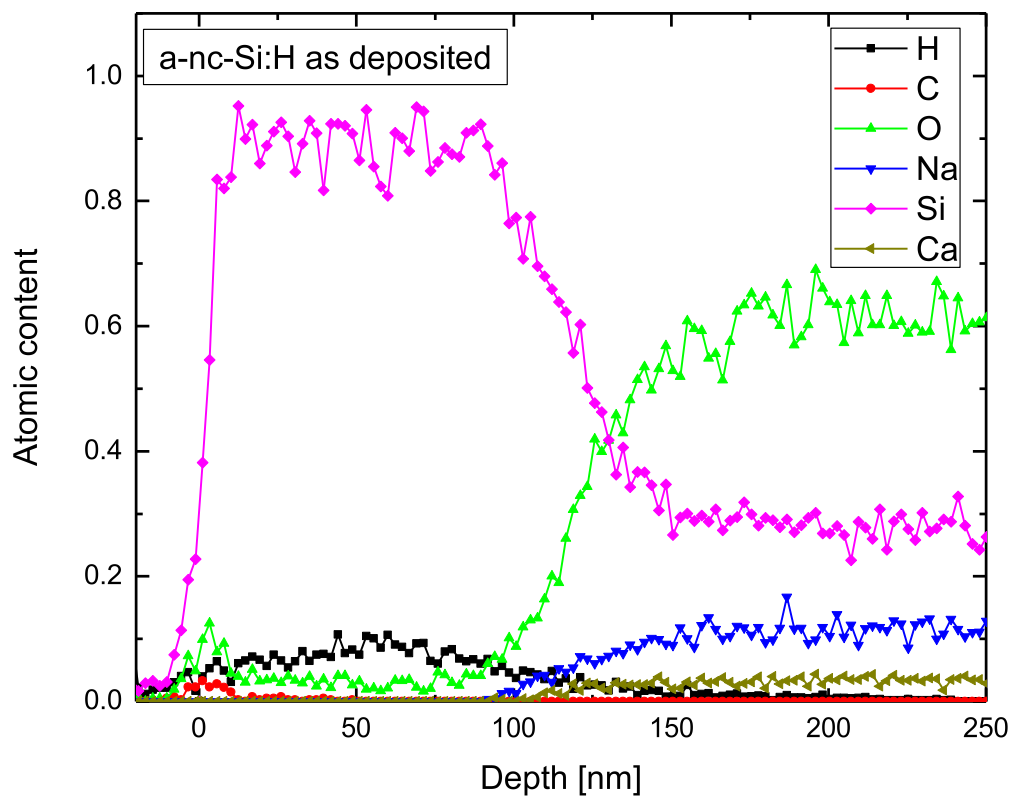


Fig 7a

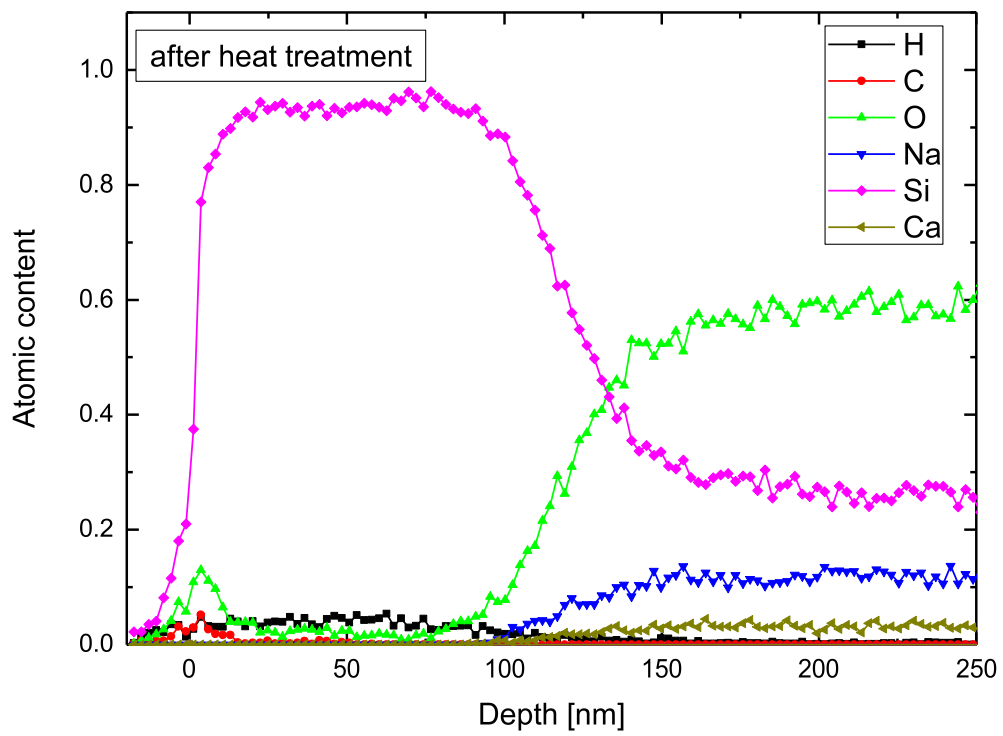


Fig 7b



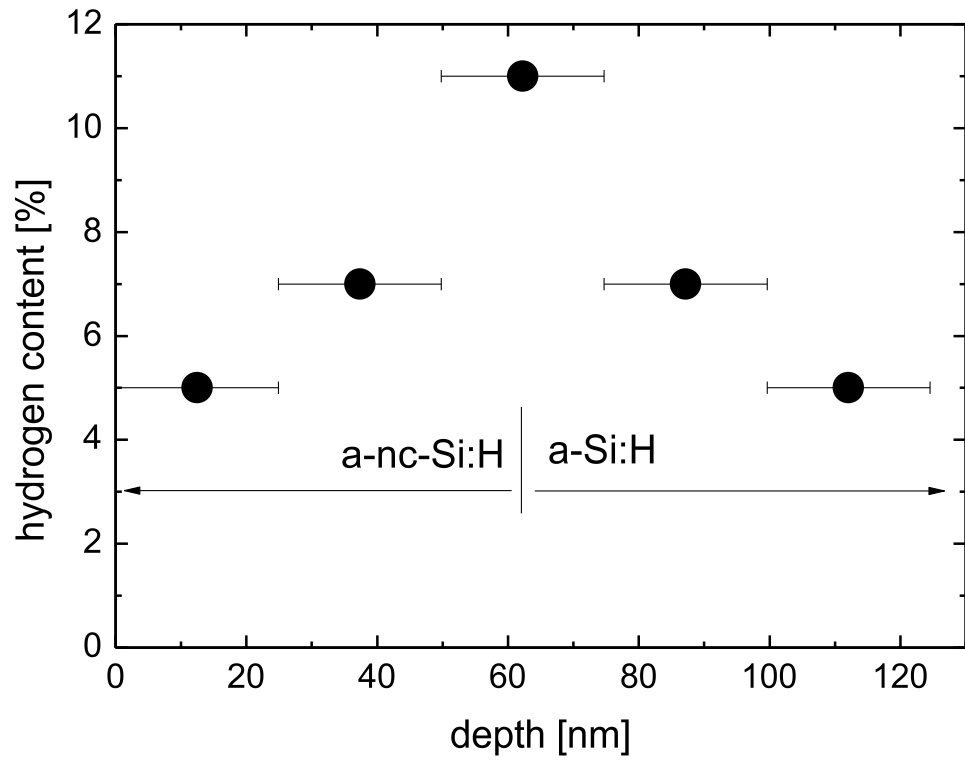


Fig 8a

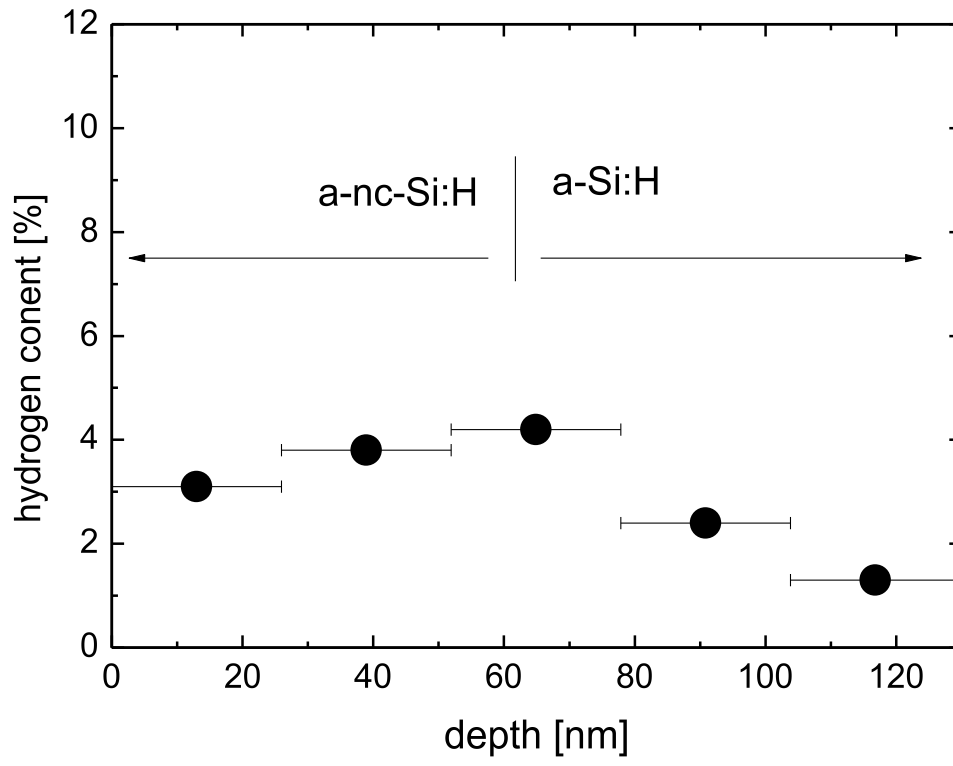


Fig 8b